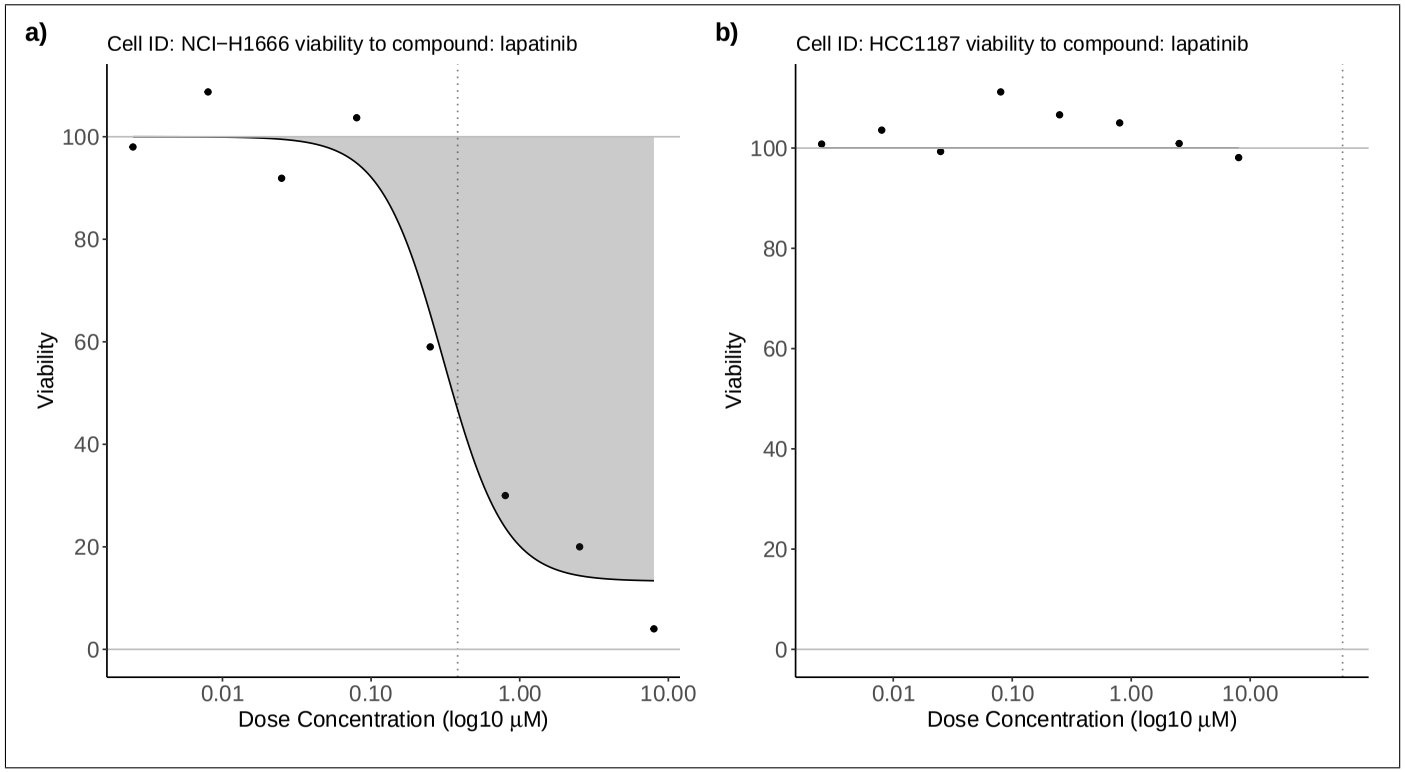

Fig. 1. Summarizing dose response. Quantification of cell response to treatment is obtained from a dose-response curve in which variable dosage concentrations are administered and the cell relative viability (relative to control wells, viability depicted on Y-axis) is recorded at each dosage concentration (X-axis). Lower relative viabilities will be observed for cells exhibiting high sensitivity to a drug (**a**) whereas relative viability will remain near 100% for cells exhibiting little-to-no sensitivity to the drug. A dose-response curve may then be estimated from the relative viabilities and summarized with 1) the half maximal effective concentration (EC50; the dose concentration level at which the curve crosses 50% viability), or 2) the half maximal inhibitory concentration at which 50% of the maximum response is attained (IC50, vertical dotted line) or 3) by computing the area-above-the-curve and normalizing to a range of zero to one (grey shading in **a**). Highly sensitive cells will attain higher values of area-above-the-curve (**a**, AAC=0.36) while resistant cells will have low values of AAC (**b**, AAC=0). Similarly, highly sensitive cells will attain smaller values of EC50/IC50 but these quantities may be unbounded for resistant cell lines due to estimation of the dose-response curve (**b**, EC50=∞).

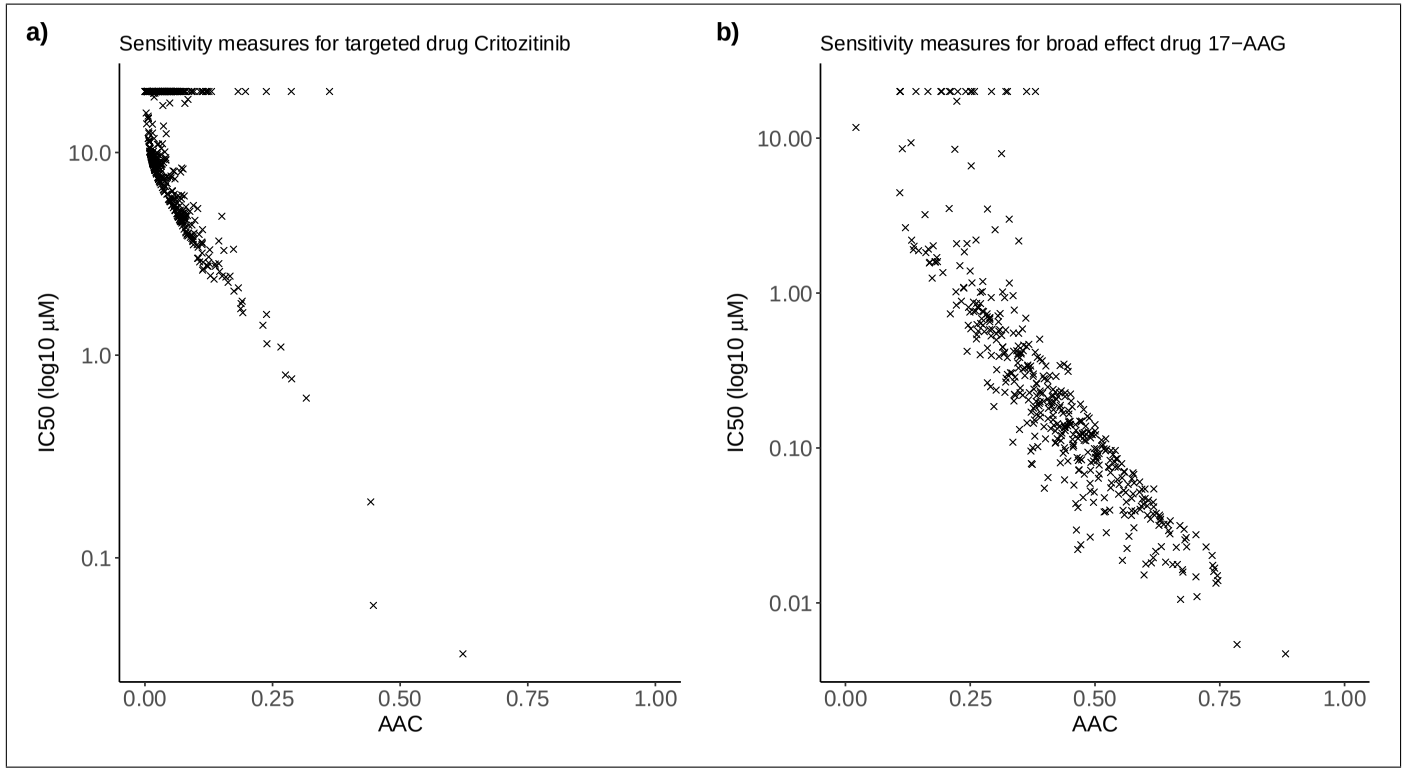

Fig. 2. Alternative dose response summary measures. In the cases of highly targeted drugs such as Crizotinib (**a**) few cells will be sensitive to treatment and therefore attain high values of AAC (X-axis) and low values of IC50 (Y-axis). The majority of the cells will be resistant to treatment and thus attain low values of AAC and high values of IC50. Binarization of cells into sensitive and resistant groups would appear appropriate in these cases. On the other hand, in the cases of broad effect drugs such as 17-AAG (**b**), nearly all cells exhibit some degree of response by both summary measures and sensitivity is best modelled by a single continuous distribution rather than binarization. IC50 values were capped at 20 prior to computing the log for visualization purposes.

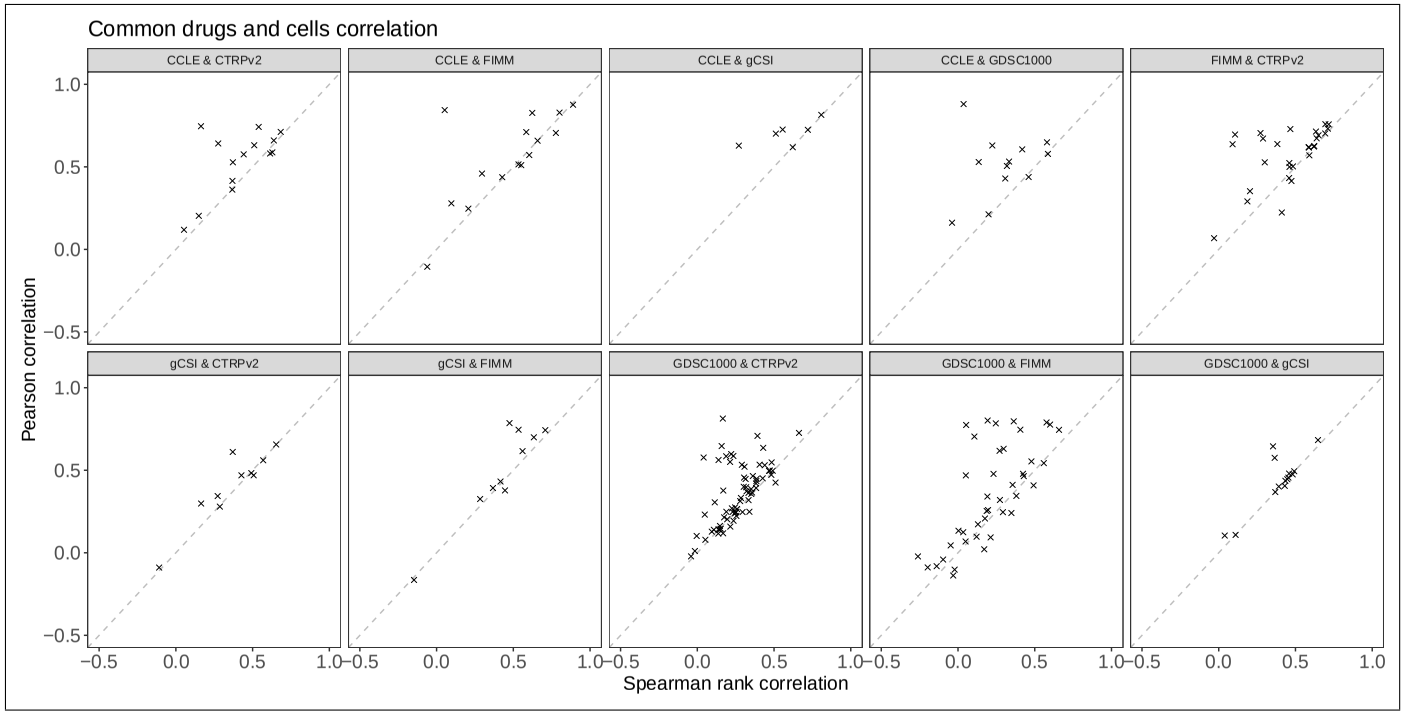

Fig. 3. Common drugs and cells correlation. Spearman rank correlation (X-axis) and Pearson correlation (Y-axis) for cells and drugs present in at least two datasets. Each point represents a single drug, with the correlation computed based on AAC values calculated over a common range.

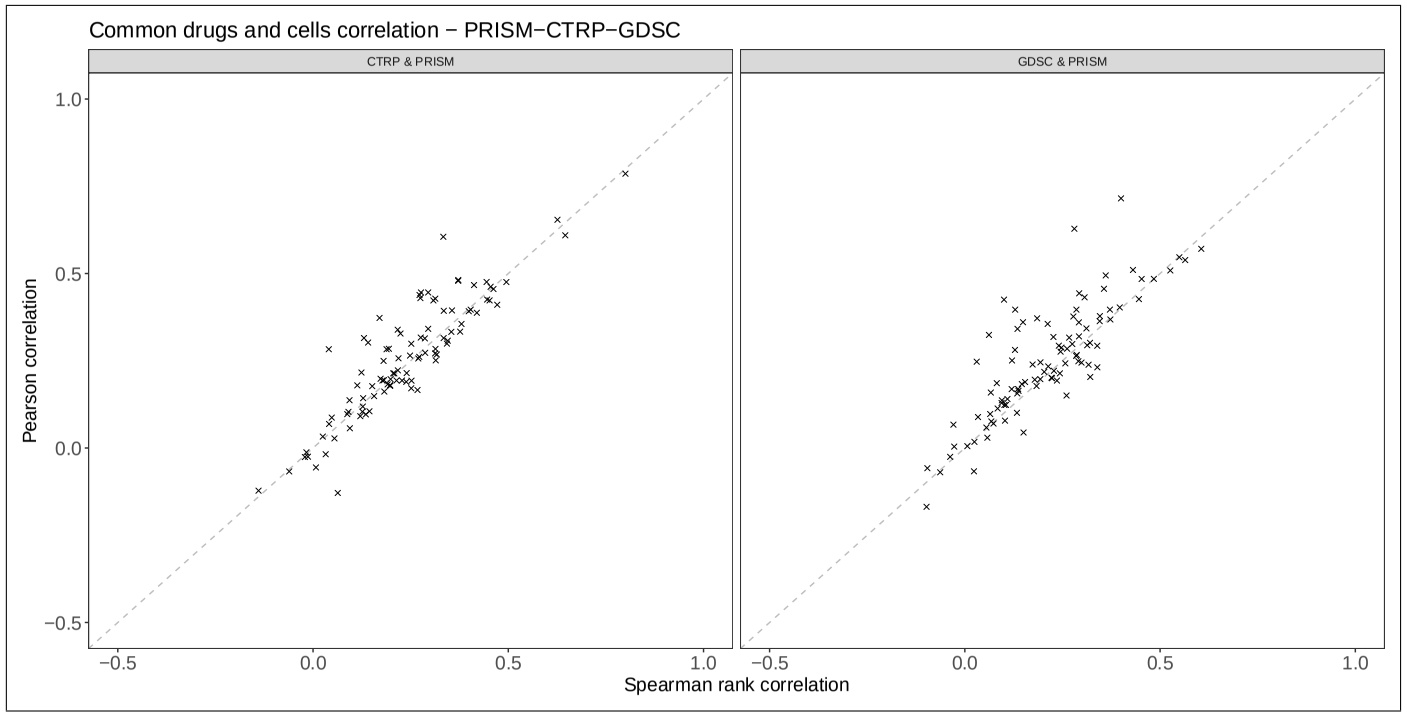

Fig. 4. Common drugs and cells correlation with PRISM. Spearman rank correlation (X-axis) and Pearson correlation (Y-axis) for cells and drugs present in the PRISM dataset and either the CTRP (left panel) or GDSC dataset (right panel). Each point represents a single drug, with the correlation computed based on AAC values calculated over a common range. Less than five drugs were tested in both the FIMM and PRISM dataset, as with gCSI/PRISM and CCLE/PRISM, and were thus excluded.

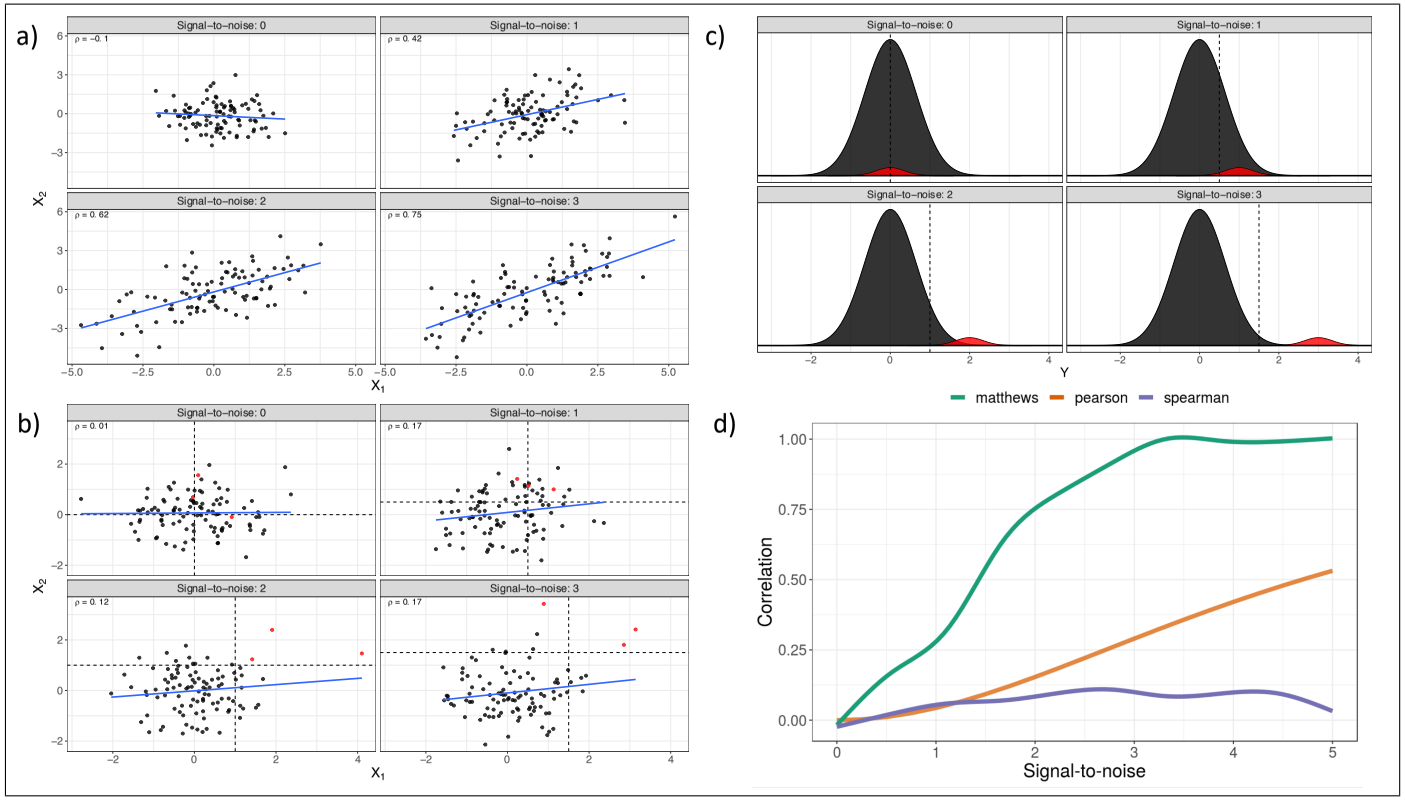

Fig. 5. Agreement for bivariate two-component mixture distributions. **a)** Two normally-distributed random variables X_1 and X_2 which follow a bivariate normal distribution. Four signal-to-noise regimes depict the relationship between the signal-to-noise ratio (covariance divided by uncorrelated variance) and the Pearson correlation (covariance divided by total variance). A single simulation repetition is pictured. **b)** Two random variables which instead follow a bivariate two-component mixture of normals. Color indicates mixture membership and dashed lines denote one-half the signal, a naïve method for classifying points to a given mixture and used for calculating Matthew's binary correlation. **c)** The generating mixture distributions under the same four signal-to-noise regimes. Signal is defined as the distance between the means of the distributions and noise is the total uncorrelated variance. Again dashed lines represent one-half the signal. **d)** Three measures of agreement (Pearson correlation, Spearman rank, and Matthew's correlation) for two random variables simulated from the generating distributions in c. Pearson correlation is derived analytically (see Supplementary Methods) while Matthew's correlation and Spearman rank are smoothed across five repetitions.

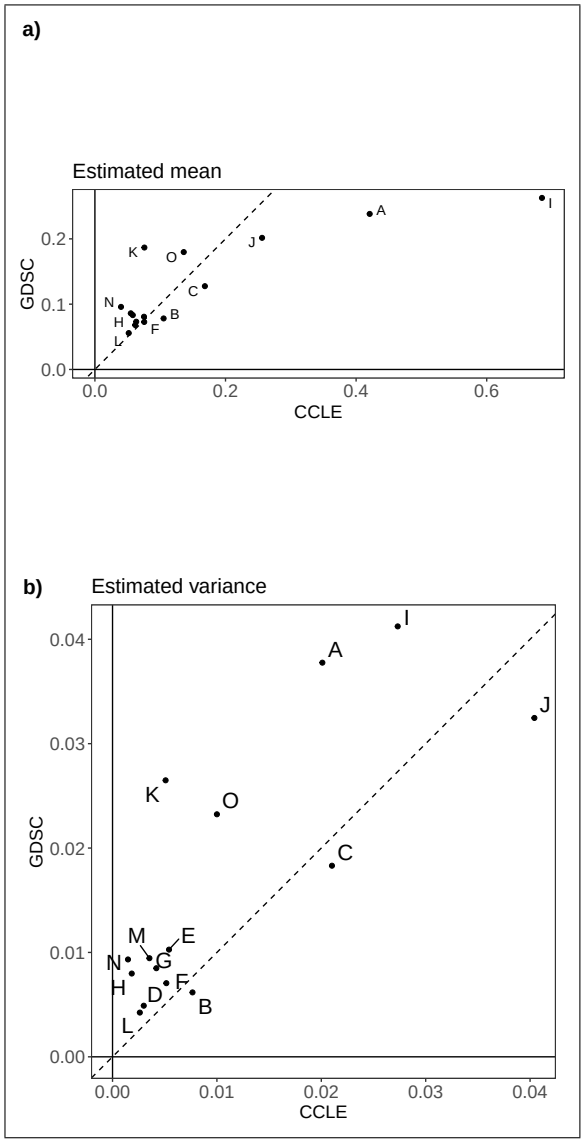

Fig. 6. Estimated mean and variance for common drugs in CCLE AND GDSC. Estimated mean AAC (**a**) and variance (**b**) from fitting single component beta distributions to compounds tested in both CCLE (X-axis) and GDSV (Y-axis). AAC values computed over similar dosage range. Common drugs include A:17-AAG, B:AZD0530, C:AZD6244, D:Crizotinib, E:Erlotinib, F:lapatinib, G:Nilotinib, H:Nutlin-3, I:paclitaxel, J:PD-0325901, K:PD-0332991, L:PHA-665752, M:PLX4720, N:Sorafenib, O:TAE684.

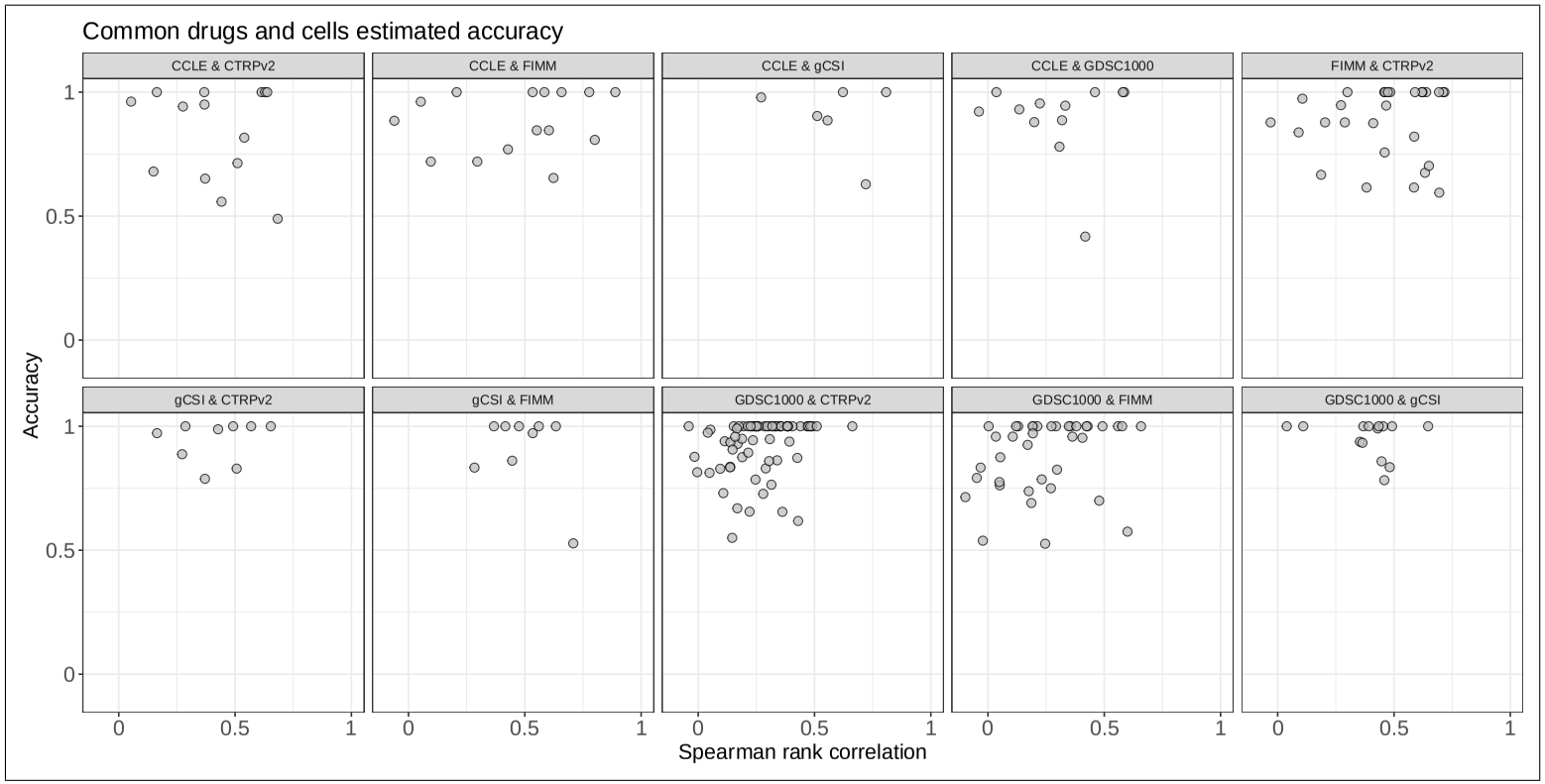

Fig. 7. Spearman rank correlation (X-axis) and accuracy (Y-axis) for cells and drugs present in the intersection of any two datasets (CCLE, GDSC1000, gCSI, FIMM, CTRPv2). Each point represents a single drug, with the agreement compute hd based on AAC values calculated over a common range. Each panel displays a pairwise comparison.

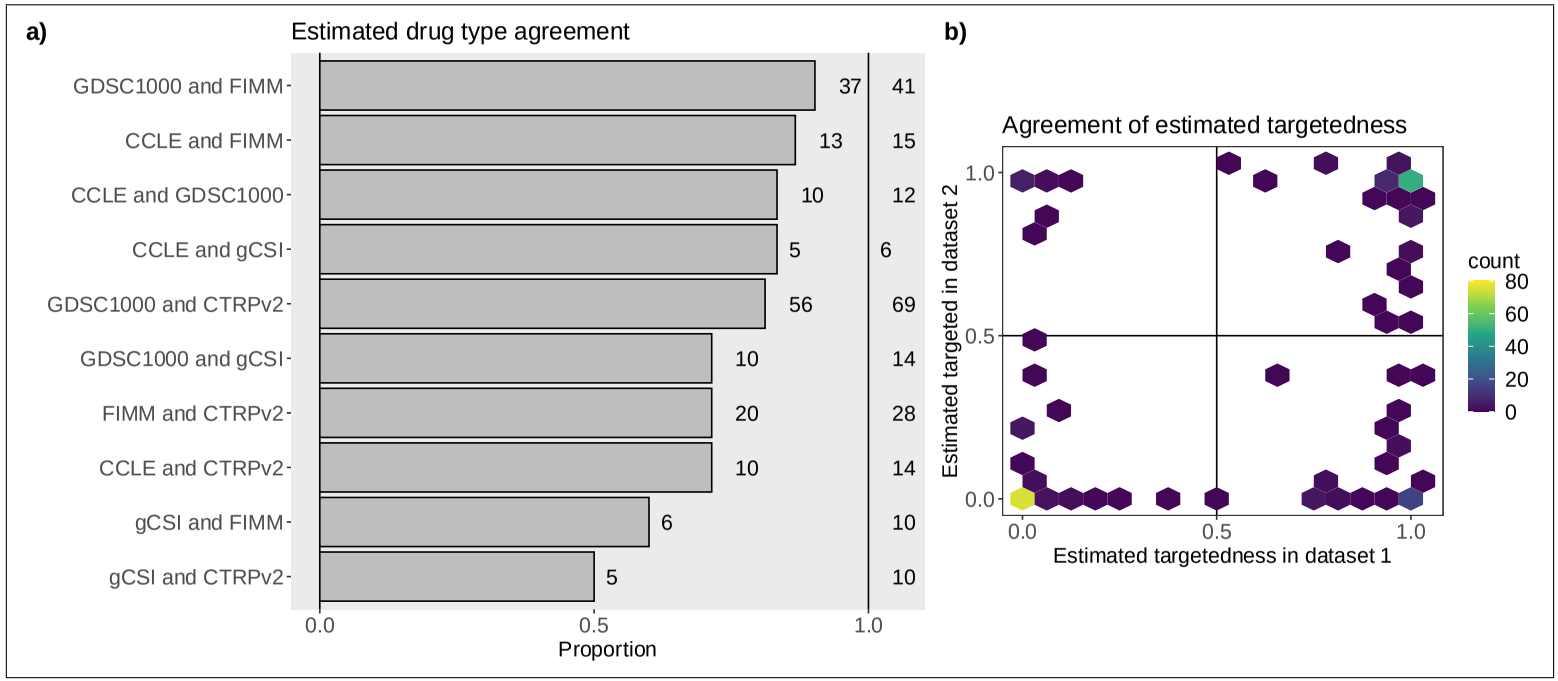

Fig. 8. Estimated pairwise drug type agreement between all datasets. **a**) The proportion of drugs with the same estimated drug type for drugs present in the intersection of any two datasets (CCLE, GDSC1000, gCSI, FIMM, CTRPv2). The numbers indicate the raw counts. **b**) Estimated drug targetedness for all drugs present in any two datasets; drugs estimated to be more broad effect in both datasets will lie in the lower left corner, whereas drugs estimated to be more targeted in both datasets will lie in the upper right corner. Drugs exhibiting low drug type agreement lie along the off-diagonals. The fill represents the total count of drugs within the bin.

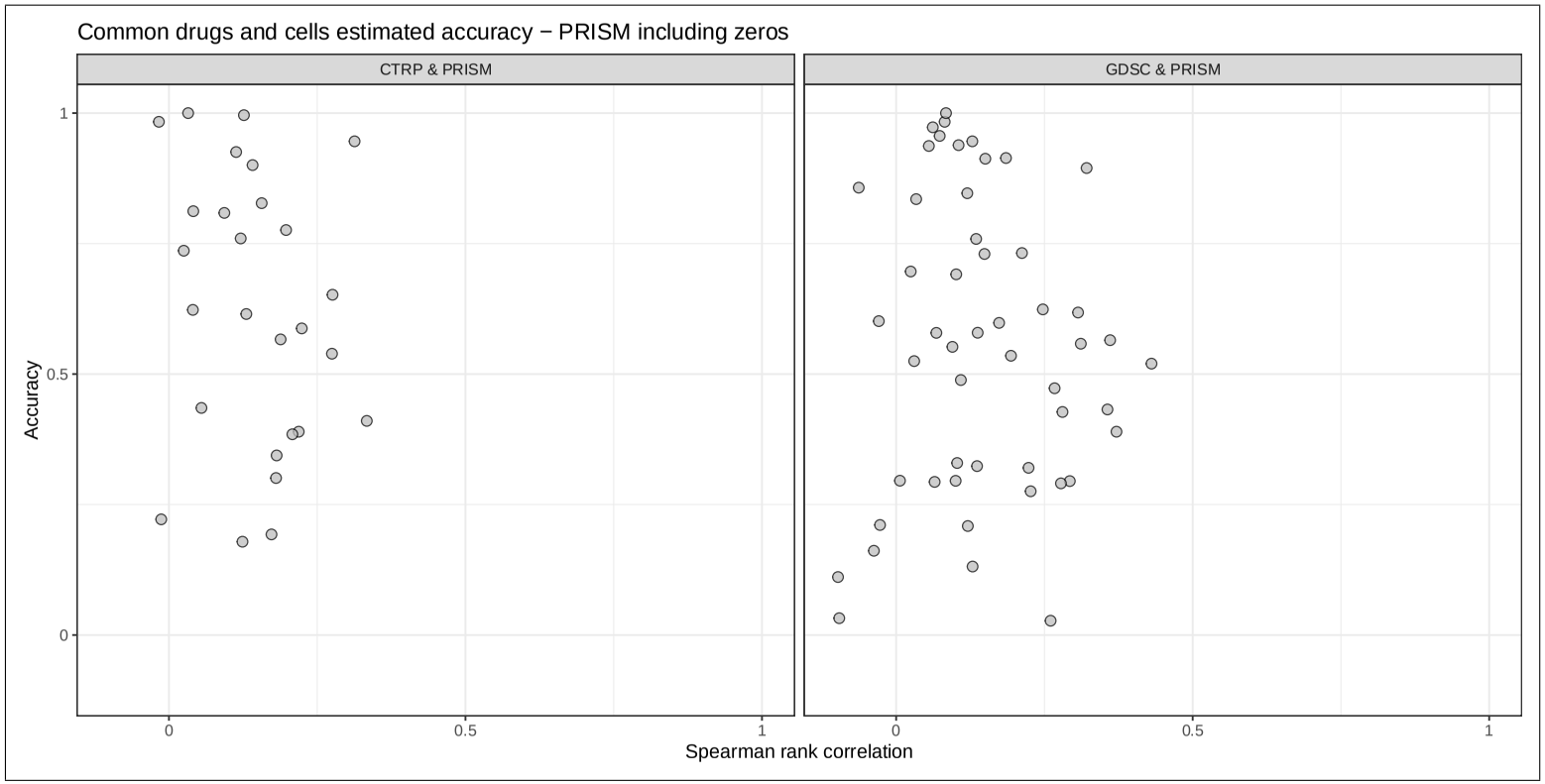

Fig. 9. Targeted drug accuracy in PRISM including non-responsive cells. Spearman rank correlation (X-axis) and accuracy (Y-axis) for cells and drugs present in the intersection of the PRISM dataset and either the CTRP dataset (left panel) or the GDSC dataset (right panel). Each point represents a single targeted drug, with the agreement computed based on AAC values calculated over a common range.

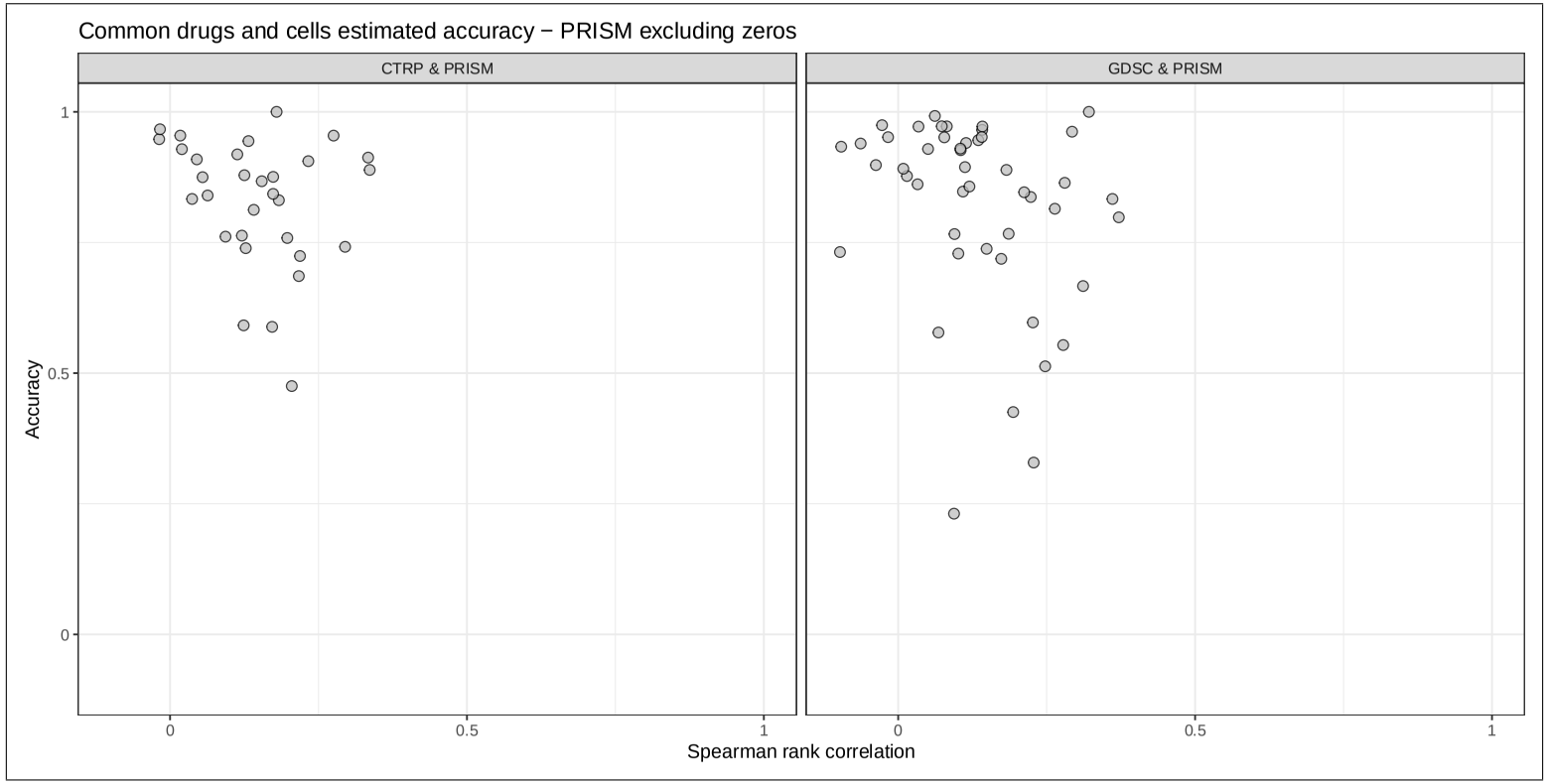

Fig. 10. Targeted drug accuracy in PRISM excluding non-responsive cells. Spearman rank correlation (X-axis) and accuracy (Y-axis) for cells exhibiting positive response (AAC > 0) and drugs present in the intersection of the PRISM dataset and either the CTRP dataset (left panel) or the GDSC dataset (right panel). Each point represents a single targeted drug, with the agreement computed based on AAC values calculated over a common range.